

Role of the friction layer in the high-temperature pin-on-disc study of a brake material

Piyush Chandra Verma¹, Rodica Ciudin¹, Andrea Bonfanti², Pranesh Aswath³,
Giovanni Straffelini¹, Stefano Gialanella^{1*}

1: Dipartimento di Ingegneria Industriale, Università di Trento, via Sommarive 9, 38123, Povo, Trento Italy.

2: Brembo S.p.A. Via Europa, 2, 24040 Stezzano (Bg), Italy

3: College of Engineering, University of Texas at Arlington, 416 Yates Street, Rm. 624
Arlington, TX 76019, USA

* : corresponding Author – stefano.gialanella@unitn.it

Abstract:

The tribological behavior of a commercial brake pad material, wear tested under dry sliding conditions against a cast iron counterface disc with a pin-on-disc apparatus, was investigated. Wear tests were conducted at the following disc temperatures: 25°C, 170°C, 200°C, 250°C, 300°C and 350°C. Above 170°C a transition from mild to severe wear was observed. At 25°C and 170°C, the friction layer on the pin surface consists of primary and compacted secondary plateaus. At 200°C and above, a progressive reduction of the pin surface coverage by the secondary plateaus, that are barely present after the 350°C test, is observed. Wear tracks on the discs derive from wear fragments due to the tribo-oxidation of the disc itself and from the wearing out of the pin material. The observed tribological behavior is very much influenced by the thermal degradation of the phenolic binder of the friction material, confirmed by thermogravimetric analyses, conducted on purpose on the pin material. Raman spectroscopy indicated the presence of carbonaceous products on the high temperature worn out pin surface. Although referring to rather extreme conditions and simplified sliding conditions, the results obtained in this study provide useful indications on the role of the thermal stability of the organic component.

Keywords: High-temperature wear tests; friction coefficient; severe wear; mild wear; brake materials; degradation phenolic resin.

1. Introduction

Brake materials transform the kinetic energy of the vehicle into thermal energy by friction between pad materials and metal, usually cast iron, disc [1]. Heat is then dissipated through exchange mainly with the environment and during braking, temperature may even rise tremendously in the contact regions. Wear behavior at the elevated temperatures resulting from the braking conditions, is highly dependent on the ingredients of the friction materials. These are to be selected in order to guarantee suitable braking conditions, high temperature stability and, consequently, reduced wear rates. However, at high temperatures, the degradation of friction material is a major issue, mostly associated with the thermal decomposition of phenolic resins, widely used as binders for friction materials [2-4]. They embed the ingredients effectively over most of the operational regimes, thanks to a good combination of mechanical properties, such as high hardness, compressive strength, creep resistance, and very good wetting capability. However, these resins are sensitive to heat and humidity, which cause serious threat to frictional, wear behavior at elevated temperatures, notwithstanding the common practice to add to the formulation suitable, carbon-based stabilisers, like graphite, coal, etc. [5-6]. Therefore, binder decomposition is blamed for various brake operational drawbacks, with specific studies displaying the importance of the heat resistance and mechanical strength of the binder in the wear behavior of brake materials.

Thermal decomposition of the phenolic resins involves several reactions, depending on the actual formulation and thermal history of the material. Temperatures falling in the 250°C - 475°C interval are reported for the onset of the main transformations involved with the resin decomposition [7-8]. Another important aspect affecting the tribological behavior of sliding wear systems is the trapping of wear debris in between the sliding surfaces [9-13], leading to the formation of the so-called friction layer, or friction film, that is paramount in determining the friction behavior of the mating surfaces in sliding contact [14-17]. Jacko et al. [18] concluded that “when stable friction films, commonly called friction layers, are readily formed for a given friction couple, a stable friction level and low wear rates can be maintained at various temperatures, as long as the friction film is not destroyed”. The wear processes, that occur at the pad and disc interface, display several steps, including the formation of the primary plateaus, formed by tough metallic fibers and coarse, hard particles (see Fig. 1); and secondary plateaus, that build up for the compaction of the wear debris blocked by the primary plateaus. The wear behavior of brake systems is thus influenced by the formation of the friction layer [3,14], its transformation related to its compactness and thickness, and, finally, by its possible detachment with consequent release of fragments and wear debris [15, 17,19-20].

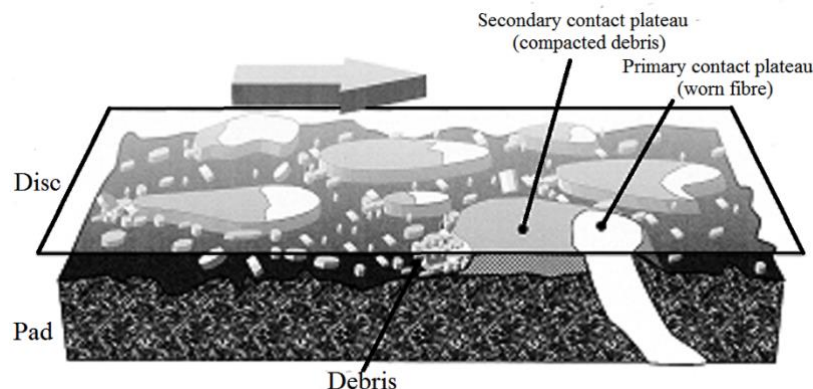


Figure 1: Schematic of the contact situation between an organic friction material and a brake disc and formation of compacted plateaus [18].

In this context, Verma et al. [21] reviewed the frictional behavior of a commercial low-steel pad material dry sliding against a cast iron disc at room temperature under mild wear conditions, using pin-on-disc wear tests. The formation of primary and secondary plateaus was observed. Two main kinds of secondary plateaus were identified: well compacted plateaus rich in copper, zirconium and iron oxide particles, forming quite large plate like fragments; less compacted plateaus, featuring a lower copper content, that tend to form comparatively smaller degradation fragments. As an extension of this former research work [21], an attempt is made herewith to investigate the friction and wear behavior of the above friction material at different disc temperatures. The degradation mechanisms observed in the friction material induced a transition from mild to severe wear during continuous dry sliding conditions. Through this study, it was possible to gain further information on the main wear mechanisms and in this way to identify critical parameters to develop better friction materials, in the context of performance, lifetimes and pollutant emissions.

Of course, this is just the first step forward. The indications obtained from the pin-on-disc lab tests require extension and validation through additional measurements carried out using experimental apparatuses, e.g., dynamometer rigs, better reproducing real brake conditions.

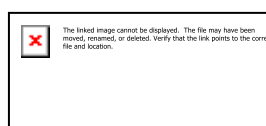
2. Experimental Details

2.1. Friction material

The elemental composition of the friction material, as measured by X-ray fluorescence (XRF) spectroscopy is shown in Table 1a. Fig. 2 shows the microstructure of the starting friction material and the main identified phases in the pad materials are listed in Table 1b. Relevant phase concentrations were calculated from XRF data (Table 1a), with the help of stoichiometry. Further details concerning the characterization of the friction material, that is being investigated as a reference in the framework of a broad research project aiming at reducing particulate matter brake system emissions, can be found in [21] The thermal degradation of the friction material was studied using a Netzsch JUPITER STA 449 F1 thermobalance. The tests were carried out at a constant heating rate of $10^{\circ}\text{C min}^{-1}$ from room temperature up to 1050°C under a nitrogen (50 ml min^{-1}) and oxygen (20 ml min^{-1}) mixed flux, simulating an “*air atmosphere*”.

2.2. Test procedure and high temperature setup

In this study, dry sliding wear tests were carried out using a pin-on-disc rig. The disc was made of pearlitic-bainitic gray cast iron with a hardness of $350 \pm 11\text{ HV}_{60}$. The cylindrical pins ($\text{Ø } 5.5\text{ mm} \times 7.7 \pm 0.3\text{ mm}$ height) were extracted from the above commercial low-steel friction material. The dimensions of the pin, particularly its diameter, if compared with the microstructure of the friction material (Fig. 2), can be safely regarded as representative of the actual material properties. The pins were abraded on the bottom side, opposite to the test surface with a SiC 800 grit abrasive paper to render this surface planar for a better thermal contact with the pin-holder and a conformal contact with the disc. The wear of the pin was measured by checking its weight before and after each test, using an analytical balance with a precision of 10^{-4} g . Data were then converted into wear volumes using a measured density of the friction material, equal to 2.27 g/cm^3 . The specific wear volume, W , was calculated from the following relation, eq. 1:



(1)

where: W_1 and W_2 are the weights of the pin before and after the test respectively, ρ is the density of the friction material and d is the sliding distance. From W , the specific wear coefficient, K_a , was determined, using eq. 2 :

$$K_a = W/F \quad (2)$$

where F is the applied load. The disc wear was measured with a profilometer, used to evaluate the cross section of the wear trace. During each test, the friction coefficient was continuously recorded together with the evolution of the pin-disc contact temperature. For this purpose, two chromel-alumel-type thermocouples were placed in two holes drilled in the pin holder at a distance of 4 mm and 6 mm from the contact surface with the disc. To estimate the average contact temperature, the frictional heat flow was considered to be one-dimensional and temperature was then assumed to decrease linearly from the contact surface upward.

Elements	wt %	Component	% wt
Mg	1.2	Zirconia (ZrO ₂)	31
Al	2.5	Al & Mg oxides	9.5
Si	2.1	Iron (Fe)	8
Zr	26.9	Copper (Cu)	7.5
S	1.8	Vermiculite	6
K	3.1	Barite (BaSO ₄)	5
Sn	2.4	Potassium Titanate (K ₂ O.6TiO ₂)	5
Ca	3.2	Alumina (Al ₂ O ₃)	3
Ti	8.3	Calcite (CaCO ₃)	2.5
Fe	6.1	Tin Sulphide (SnS)	2.5
Cu	8.1	Zinc (Zn)	2
Zn	3.1	Bismuth (Bi)	0.6
		Iron Sulphide (FeS)	0.5
		Rest (phenolic resin, graphite, etc.)	

a)

b)

Table 1: Elemental composition of the friction material (No carbon and oxygen quantification) (a). Concentrations of the compounds present in friction material (b).

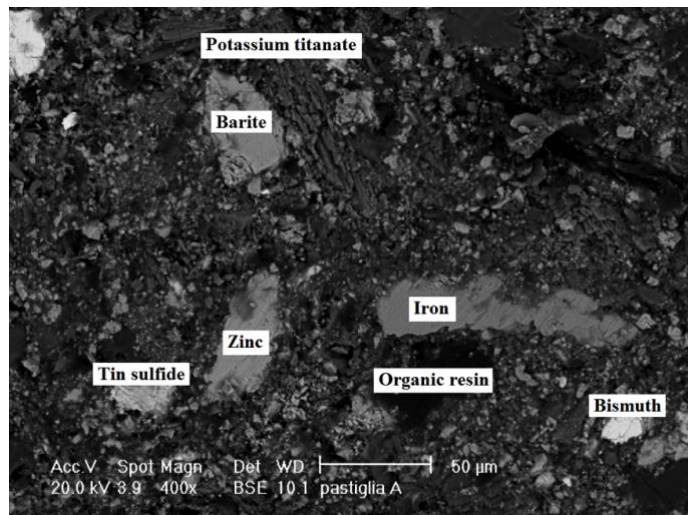


Figure 2: Microstructure of starting friction material with the indication of the main component phases.

The tests were carried out with a laboratory high temperature pin-on-disc rig, at the following controlled disc temperatures, starting from room temperature (25°C), 170°C, 200°C, 250°C and 300°C. A test was also conducted at 350°C but stopped before completion, since excessive wear rate would have not allowed the test to run for the full duration. However, the pin and disc from this interrupted test were analyzed and provided results interesting for a better understanding of the wear behavior of the system at elevated temperatures. Temperatures were selected on the basis of the thermogravimetric results. It is interesting to note that car brake peak temperatures can achieve 200 °C in particularly severe conditions. The other conditions of the tests were: sliding speed of 1.31 m/s (corresponding to 500 rpm), applied pressure of 2MPa and actual sliding distance of 4000 meters, for a total duration of 50 min. per test. At the beginning of each test, a 10 min run-in period was allowed to attain a stable contact between pin and disc. The pin-on-disc apparatus was equipped with an external heater of the disc, which enables wear tests to be conducted at temperatures as high as 1000°C.

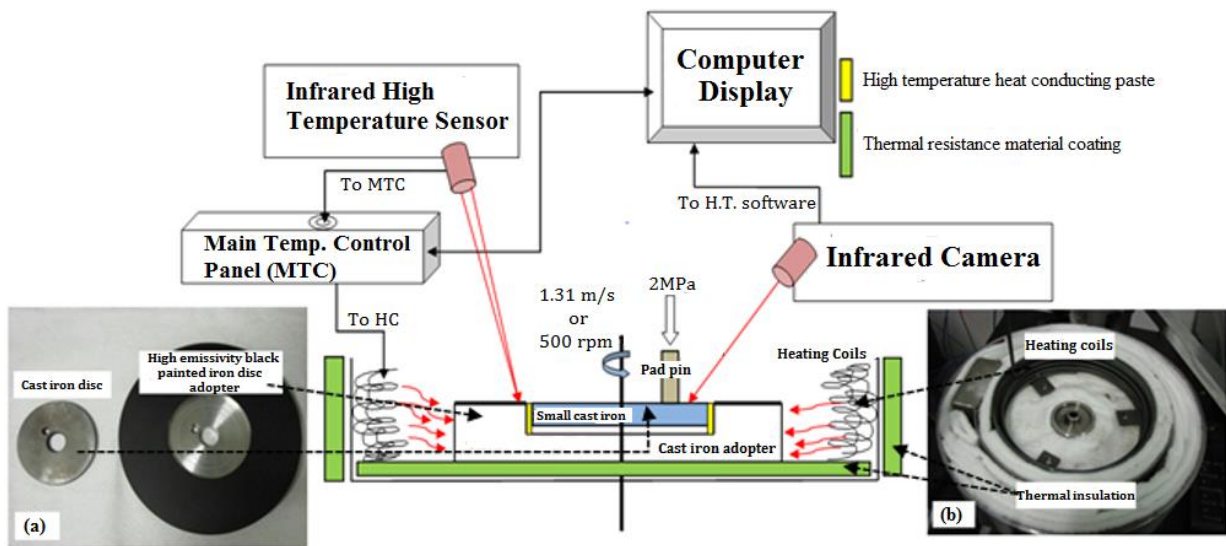


Figure 3: Schematic closed loop feedback high temperature wear test setup.

Fig. 3 shows the schematic of the high temperature wear test arrangement, which is a closed loop feedback system, in which the temperature of the cast iron disc (Fig. 3, inset a) was maintained at the set value by the *heating coil* (HC) (Fig. 3, inset b) that is governed by the *Main Temperature Control* (MTC) panel through an infrared high temperature sensor and a thermal camera (Fig. 4). **In this way it was also possible to compensate for the temperature raise due to frictional heating.**

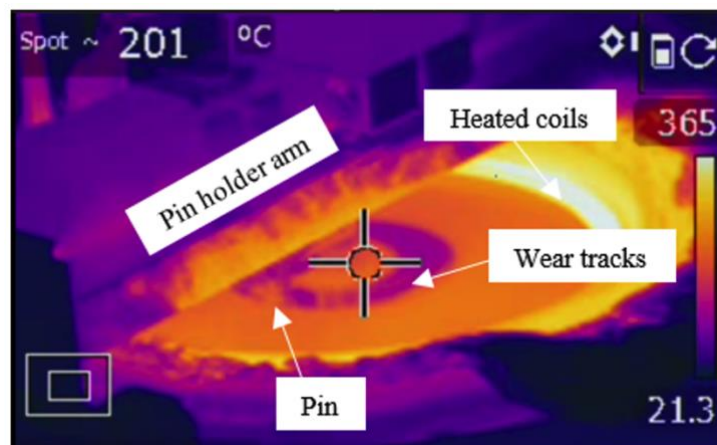


Figure 4: Infrared camera snapshot of the wear test at 200°C.

A cast iron disc with a 63 mm diameter was fitted into the groove of a cast iron adapter (diam. 140 mm) (Fig. 3, inset a). The upper surface of the adapter, surrounding the disc area, was coated with a high emissivity black paint in order to eliminate the reflection of infrared radiation from the shiny surface of cast iron. The thermal camera and infrared sensor would have otherwise measured temperature erroneously from an unpainted disc surface. The clearance between the adapter and the cast iron disc was filled with a high temperature conductive paste, which insures an adequate thermal coupling of the two parts. The high temperature pin-on-disc test rigs was wrapped with a refractory alumina felt (Fig. 3, inset b), to improve thermal insulation and to minimize heat leakage, that might damage the gears and electric motor of the pin-on-disc apparatus.

2.3. Characterization of the worn surfaces

A scanning electron microscope (SEM) equipped with an energy dispersive X-ray spectroscopy (EDXS) system was used to examine the surface morphology and composition of the worn pins and counterface discs. The Characterization of frictional material surfaces was conducted in planar and cross sectional modes. For planar view observations, samples were anchored onto microscope stubs using a double sided adhesive carbon tape, to provide an adequate electrical grounding. SEM was operated in a conventional high vacuum mode. Metallographically mounted cross sections of the pins were prepared to investigate the internal structure of the friction layer. In order to expose the section of interest, the metallographic specimens were ground and polished using silicon carbide papers of progressively finer grit. A conductive layer of carbon was deposited onto the polished surface to eliminate any charging effect. The disc surface was examined in planar view only, to investigate the microstructure and elemental composition of the transfer layer. The profile of the wear tracks on the disc surface was measured with a stylus profilometer. From this datum, the disc wear volumes were estimated from at least four measurements taken perpendicularly to the sliding direction along the disc circumference. The organic residuals from the decomposition of the phenolic resin and other components of the friction layer on the wear tested pins were characterised with Raman spectroscopy, using a Thermo Scientific DXR spectrometer equipped with a diode pumped solid-state type laser with a frequency of 532 nm and power output of 10 mW. Tests were conducted without any particular sample preparation and by selecting the region to analyses with a low magnification optical microscope. The laser spot diameter was 2 μm with 25 μm pinhole aperture, for the fully focused laser beam. The spectral resolution was 5 cm^{-1} at 532nm with a wavelength range from 150 cm^{-1} to 3500 cm^{-1} . The software program Origin Lab was used for the line profile fitting and analysis. Best fit of the curve was accomplished without fixing or limiting the range of any spectral parameters during iteration [22].

3. Results and discussion

3.1. Thermal behavior of the friction material

The thermogravimetric analysis (TGA) curve shown in Fig. 5 refers to a specimen of the investigated friction material. The thermal decomposition pathway of phenolic resins is responsible for the majority of the observed weight losses. A multistep mass loss is visible, and confirmed by the differential TG (DTG) curve. A first minor mass reduction (0.04%) appears at 90°C and major decomposition (3.77%) starts at approximately 280°C with a maximum decomposition rate at

415°C (Fig. 5), that according to literature [23-24] would be compatible with the decomposition of the phenolic binder, that proceeds by forming a char. A similar kinetics has been observed and reported already [23]: thermal decomposition of an organic friction material has given rise to a broad exothermic peak over the temperature range from 200°C to 375°C with an associated weight loss of 3-5wt% approximately.

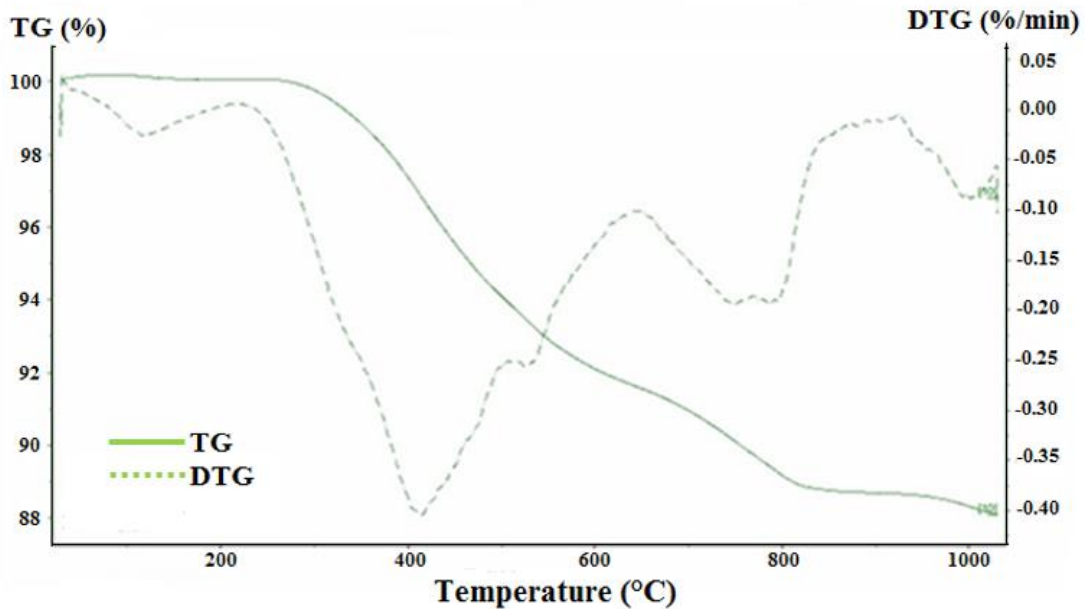


Figure 5: TG and DTG curves of friction material in air.

This is due to the oxidation and evaporation of organic components. Different studies have reported on the thermal degradation of phenolic resin at elevated temperatures [24-25]. The main components evolving during the decomposition of the phenolic resin at 230°C-450°C are H₂O and CO₂, corresponding to the decomposition of binder and oxidation of carbon [7,11]. Bijwe et al. [26] highlighted similar effects, interpreted as deterioration of resin in brake pads during the operation at 300°C - 400°C. Huong et al. [27] investigated wear of three different types of phenolic resin and observed that up to 200°C the wear process rely on breaking of hydrogen bonding, and at temperatures in excess of 300°C the phenolic resin undergoes the random scission of polymeric chains, oxidation and carbonisation, results that are in agreement with those obtained in the present study.

3.2. Friction and wear behavior

Temperature of the cast iron disc (°C)	Coefficient of friction (μ)
25	0.38 - 0.48
170	0.41 - 0.49
200	0.39 - 0.51
250	0.45 - 0.56
300	0.47 - 0.59

Table 2: Range for the friction coefficient attained after the run- in stage.

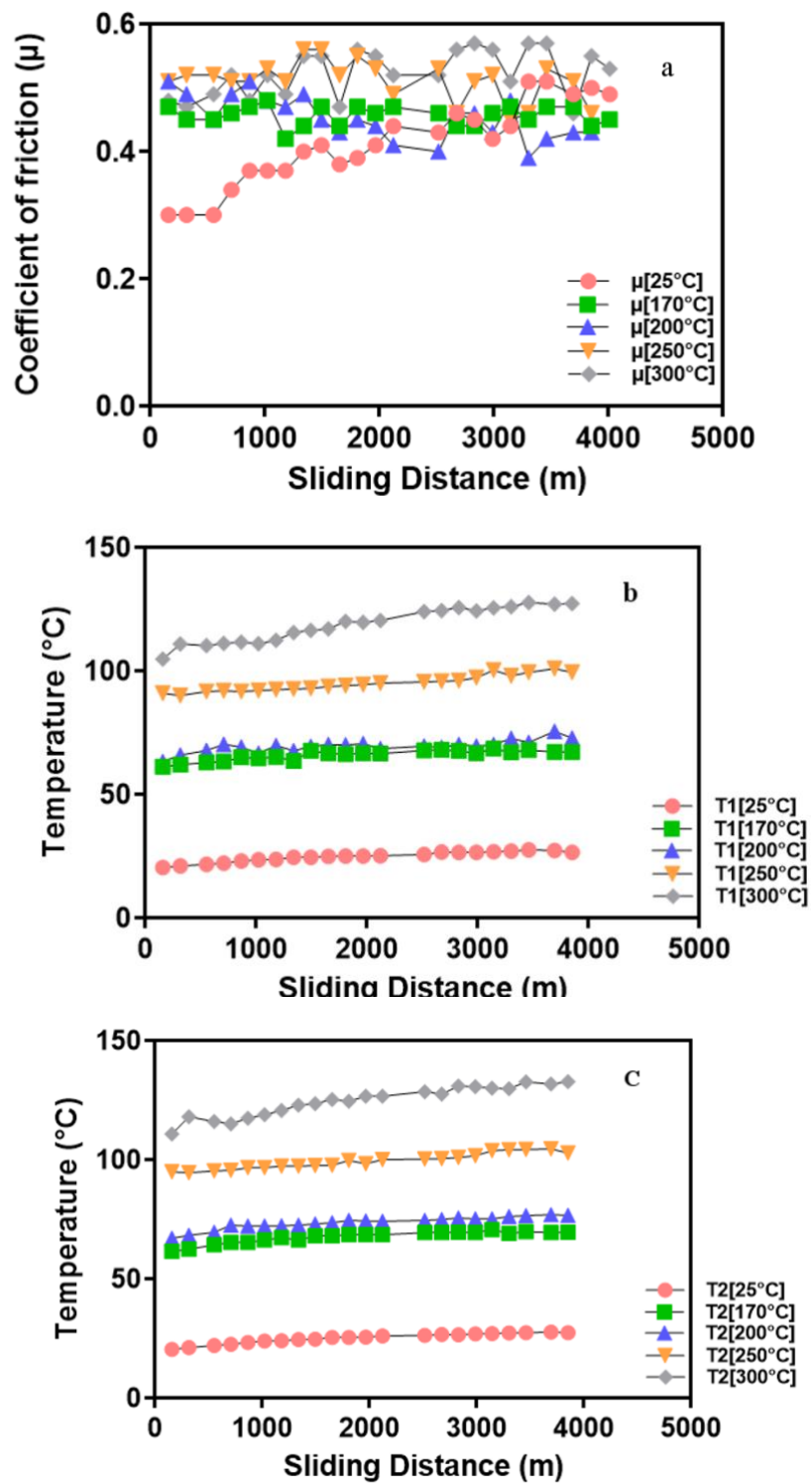


Figure 6: Evolution of the friction coefficient (a). Contact temperature of pin measured by thermocouple at 6 mm (b) and at 4 mm (c) from the disc surface.

Fig. 6a shows the evolution of the friction coefficient obtained from the pin-on-disc tests conducted at different temperatures (25°C - 300°C). The initial value of the friction coefficient for test at 25°C is close to ~ 0.38. Towards the end of the test a value of ~ 0.48 is attained. The ranges of variation for the friction coefficient at higher test temperatures are listed in Table 2. The pin temperature gradually increases with the duration of the test as measured by the thermocouples placed in the pin at 6 mm (Fig. 6b) and 4 mm (Fig. 6c) from the disc surface. The temperatures measured in the pin remain significantly lower than the disc temperatures and the contact temperatures, except for the room temperature test where the pin temperature is almost the same as the disc temperature. As a matter of fact, a sharp temperature gradient is expected to be present inside the pins, considering that the region in contact with the disc, would have the same temperature as the disc, or higher, owing to the local contribution from frictional heating. This also indicates that the thickness of the pin layer subjected to higher temperatures, because of the contact with the rotating disc, is relatively thin.

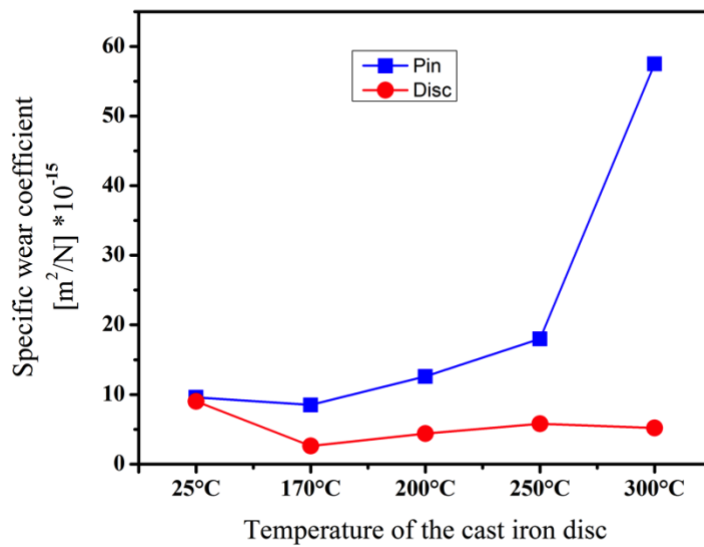


Figure 7: Specific wear behavior of pin and cast iron disc at different temperatures.

Fig. 7 shows the specific wear coefficient obtained from the pin-on-disc tests as a function of the disc temperature. Two different wear regimes can be identified for the pin. For temperatures up to 170°C, a nearly constant wear coefficient is recorded, with values that are typical of a mild wear regime. Above this temperature, a sharp change in the wear coefficient, corresponding to a sharp increase in the wear rate, drives the system into a severe wear regime. As expected, no significant change in the wear behavior of the disc is observed over the considered temperature range, which is too low to significantly affect the properties of cast iron. The only significant aspect is the slight reduction in the wear coefficient at high temperature due to the building up of a transfer layer that largely compensates for the weight loss due to the disc wear. This aspect will be considered later on in the text. The wear rates of the pin and the disc at different test temperatures are listed in Table 3.

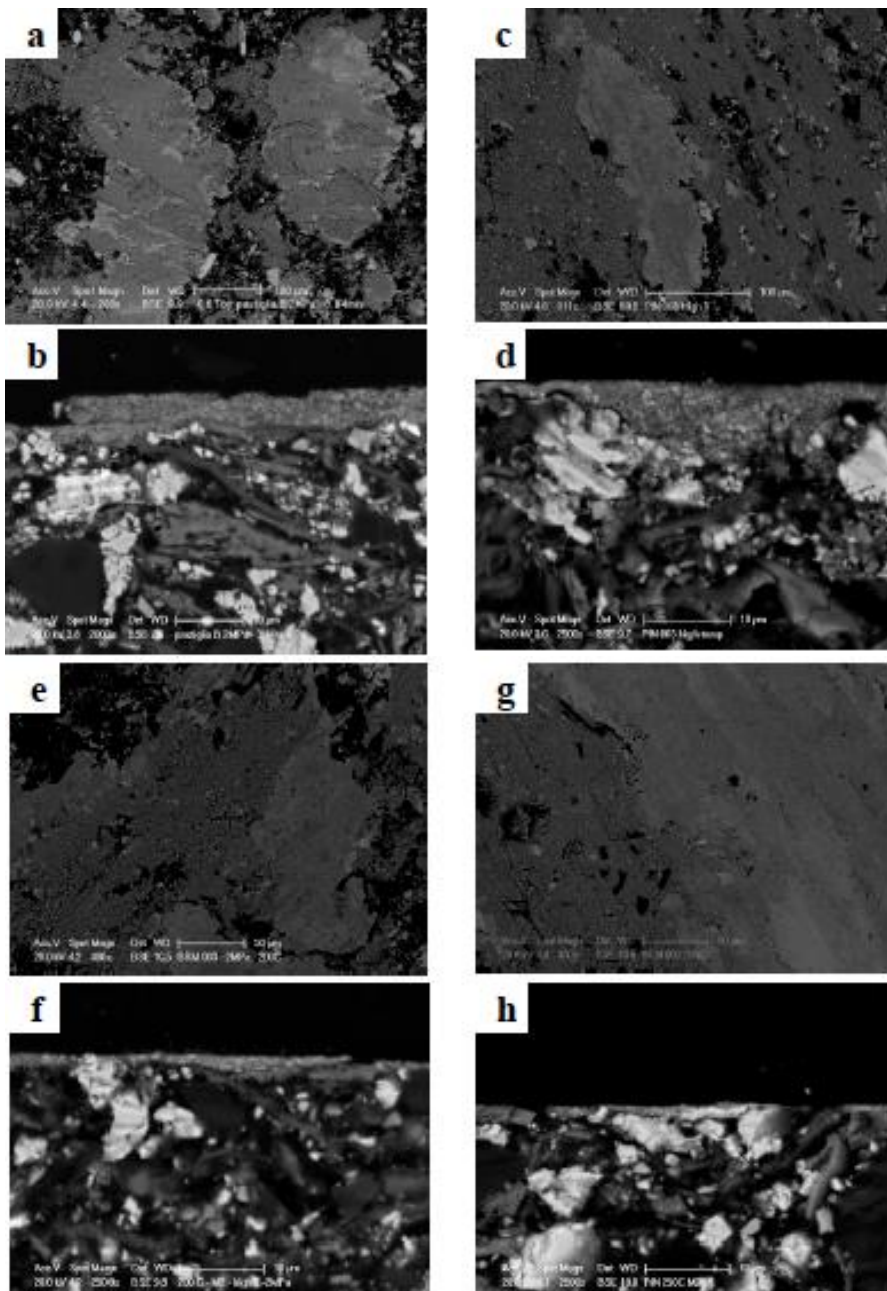
Temperature of the cast iron disc	Wear Rate [mm^3/mm] * 10^{-7}		Specific Wear Coefficient [m^2/N] * 10^{-15}	
	Pin	Disc	Pin	Disc
25 °C	4.6	4.4	9.6	9.0
170 °C	4.1	1.3	8.5	2.6
200 °C	6.1	2.1	12.6	4.4
250 °C	8.7	2.8	18.0	5.8

300 °C	27.7	2.5	57.5	5.2
--------	------	-----	------	-----

Table 3: Wear rates of the pin and the disc at different temperature

3.3. Characterization of the worn surfaces

Fig. 8 shows a complete set of SEM images of the planar and corresponding cross sectional views of the friction layers that are present on the pin worn out surfaces, after the wear tests carried out at room and higher temperatures. At room temperature and at 170°C, the pin surface exhibits good coverage by the friction layers, with relatively compact secondary plateaus (Fig. 8a and 8c). As shown by the relevant cross sectional views of the same specimens (Fig. 8b and 8d), the friction layers consist of two main components - primary plateaus and secondary plateaus, according to a well established (see Fig. 1) and already investigated pattern [21]. The primary plateaus derive from a lower removal rate of the mechanically stable and wear resistant ingredients of the pin material: hard particles and tough fibers (see Fig. 2), protruding from the surface of the pins when they start to wear out.



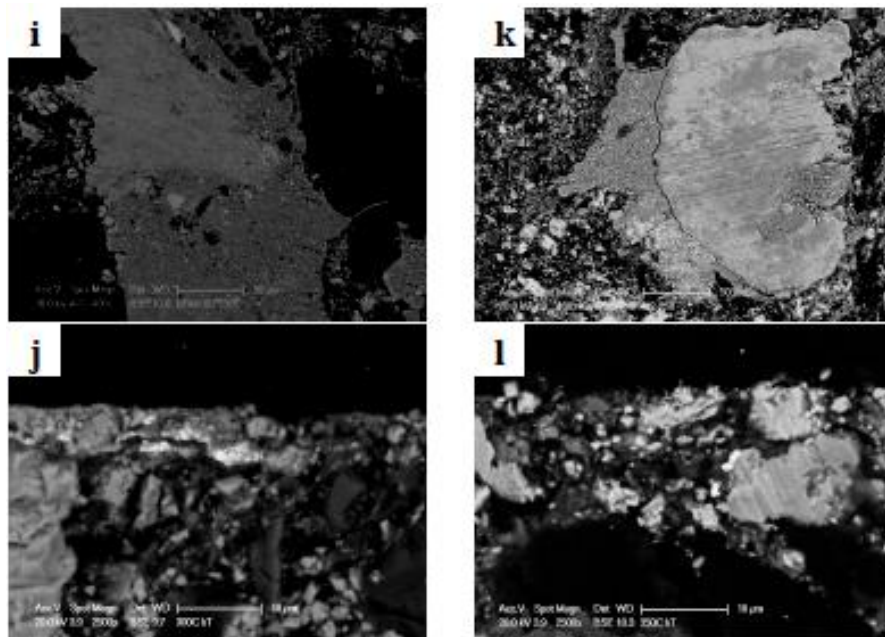


Figure 8: SEM of worn surfaces (planar view) and corresponding cross sections of surface friction layers present on the pins after pin-on-disc wear testing at the following disc temperatures: 25°C - a) and b); 170°C - c) and d); 200°C - e) and f); 250°C - g) and h); 300°C - i) and j); 350°C - k) and l).

The primary plateaus act as barriers to the movement of the finer wear particles, that therefore tend to stop and accumulate at the interface with such barriers. If these particles start to stick together, this promotes the formation of the secondary plateaus, as reported for similar systems [28-31]. The friction layer displays a progressive reduction at increasing temperatures of both the coverage of the pin surface and relevant thickness. This latter aspect is well documented by the set of SEM micrographs in Figures 8f), 8h), 8j), corresponding to samples wear tested at 200 °C, 250 °C and 300 °C, respectively. The contraction of the friction layer is significant in the secondary plateaus, that appear progressively thinner. The planar views show that residual patches of secondary plateaus, that still display regions with well compacted layers of sub-micrometric debris, also show the presence of less compacted debris and black regions, the incidence of which increases with the test temperature. In the sample tested at 300 °C (see Fig. 8j), these black regions become particularly evident and widespread on the pin surface. At 350°C, residual parts of the friction layer are hard to find and, when present, are severely damaged (Fig. 8k). The cross sectional view of this pin confirms that the secondary plateaus are nearly absent and the pin surface just features typical components of the primary plateaus, like relatively coarse ZrO₂ particles, the brighter surface grains visible in Fig. 8l. Coherent with this picture is the evolution in the friction layer composition with temperature displayed in Fig. 9, displaying a zirconium surface enrichment with the wear test temperature. The lack of extensive secondary plateaus on the surface of the samples tested at 350°C and consequent importance of abrasive processes in the wear behavior would also match with the higher friction coefficient, as displayed by the friction curve in Fig. 6a and by the data in Table 2. The friction layer that forms at room temperature is mainly made of compacted iron oxide particles, coming from the tribo-oxidation of the cast iron disc. Thinner friction layers at

higher test temperatures are compatible with a lower iron oxide concentration and increase in zirconium and copper. The spectroscopy data cannot conclusively discriminate between the two possible sources of these two elements, both of which are present in the base pin material.

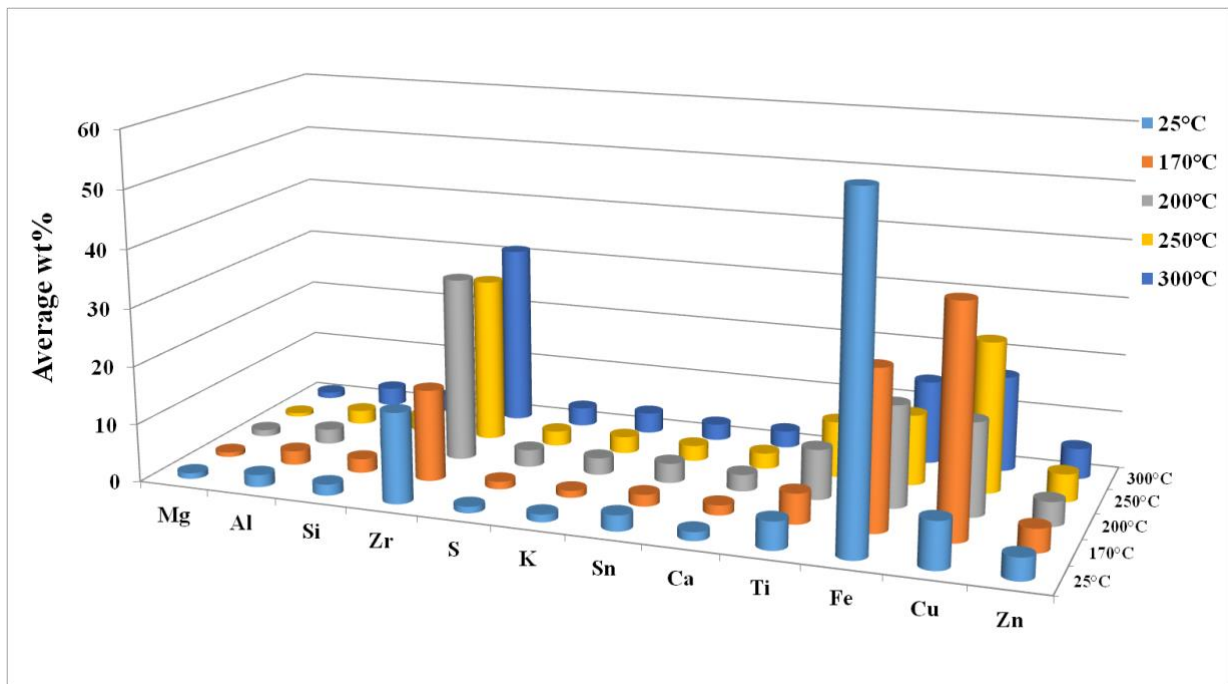


Figure 9: Average elemental composition of the friction layers present on the worn pin surfaces, as measured from EDXS spectra acquired during planar view observations.

With the reduction of the thickness of the friction layer, the inner pin volume may contribute to a larger extent to X-ray emission, than just the surface. The introduction of a hard component like ZrO_2 in the wear dynamics of the system, in view of its abrasive action, could explain the observed increase in the friction coefficient with temperature. The destabilisation of the friction layer is determined to an important extent by the presence of organic residuals accumulating on the surface of the pin. These soft organic residuals provide too a weak support for the formation of a compact and resistant friction layer. Fig. 8i) shows a fragment of the friction layer on the sample tested at 300°C, that displays a fracture right on the verge of an organic lump (black detail in the SEM picture). In this framework, copper, although present, has a reduced capability of stabilising the friction layer, as it would typically occur in this sort of tribological systems [31]. A further factor that is reducing the densification of the wear fragments, particularly those produced at the highest temperature (i.e., 350°C) is the progressive depletion of the organic components in the pin material, hence, the debris that forms during the test exhibits a lower tendency to stick together. The picture that is emerging from the data presented so far suggests that a major role in the wear behavior of the tribological system at different disc temperatures is played by the decomposition of the organic binder, for which a twofold effect can be envisaged. The degradation of the binder is affecting its ability to maintain the stability of the friction material. The friction material that is held in place by the resin is released faster when the decomposition of the inorganic components begins. The changes induced by the exposure to high temperatures, has been directly verified by Raman spectroscopy, conducted on the worn out surface of the pin materials. The Raman spectrum of the pin tested at 25°C displays a sharp peak at 1590 cm^{-1} , ascribed to polycrystalline graphite (G-component). A line is present at 1360 cm^{-1} , corresponding to the D1 component, associated to

structurally disordered graphite. A further peak, the D3 component, is present at about 1500 cm^{-1} , that is due to the presence of an amorphous carbon component [22,32]. (Fig. 10a). The formation of these carbonaceous products, considering the comparatively low temperature achieved by the pin surface (at 25°C , the measured temperature of the cast iron disc after frictional test was about 115°C) can be largely ascribed to the intense shear strain associated to the relative sliding of the pin and cast iron disc. However, also in view of the thermoanalytical data (see Fig. 5) a contribution from thermally induced structural disorder cannot be ruled out. The formation of "highly disordered graphite" is reported as a possible product of oxidation reaction of the phenolic binder [14-15]. At higher disc temperatures, e.g., 300°C , the situation evolves with the appearance of a further disorder contribution, D4 contribution at 1200 cm^{-1} approx, this time coming from the diffusion into the polymer network of ionic impurities. (Fig. 10b). This process is likely to occur considering the complex chemical environment of the system and the high operational temperature. Wear tracks present on the discs were also investigated to interpret the data in Fig. 7. They exhibit a relatively constant wear rate of the cast iron discs irrespective of the working temperature, with actually a slight reduction of wear rate at higher temperatures as compared to the room temperature value.

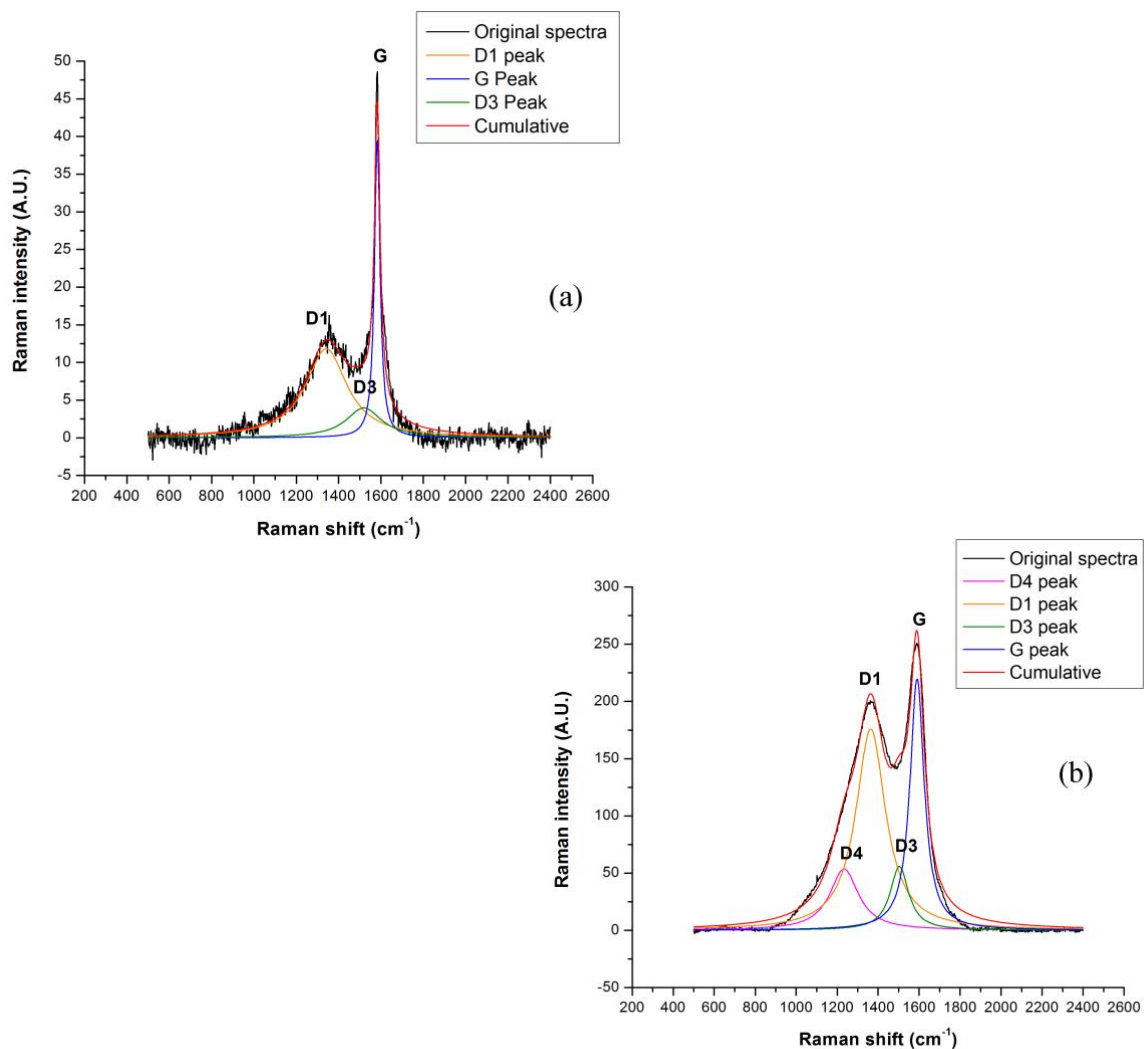


Figure 10: Lorentzian curve fit for the deconvoluted Raman spectra from friction layers present on the pin, wear tested at (a) 25°C , (b) 300°C .

Peak legend:

G (1590 cm^{-1}) band= crystalline graphite

D1(1360 cm^{-1}) band= disordered graphite structure
 D3(1500 cm^{-1}) band= amorphous carbon
 D4 (1200 cm^{-1}) band= disordered graphite due to ionic impurities diffusion

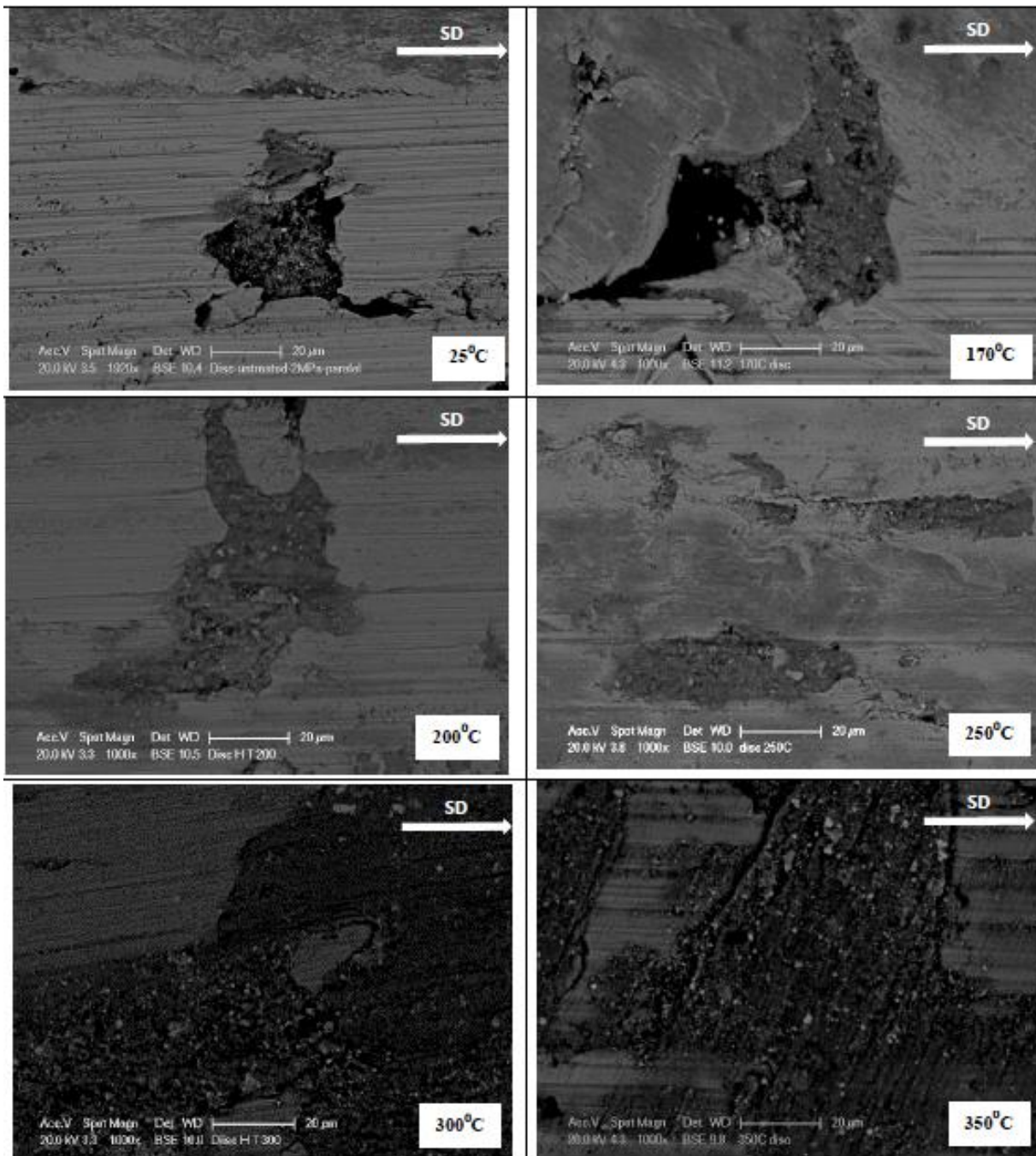


Figure 11: SEM observations of disc surface after pin-on-disc tests carried out at different temperatures, as indicated in the figure. **Note: same magnification for all micrographs.**

The SEM images in Fig. 11, displaying the disc surface for the six temperatures considered in this study, show how the wear tracks on the cast iron discs become increasingly covered with wear debris, whose composition (Fig. 12) qualitatively resembles the outer layer on the pin worn out surface (Fig. 9). This is particularly true regarding the presence of zirconium (oxide) and copper, that are coming from the pin material. However, the microstructure of these debris, particularly

those of the discs tested at 300 °C and 350°C, appear coarse grained and in this respect quite different, for instance, from the secondary plateaus on the discs and pins tested at 25°C and 170 °C. This microstructure indicates that these components are mostly released from the degrading resin and do not suffer from intense grinding associated with the relative sliding against the cast iron disc. The increasing coverage of the disc surface with wear debris is in agreement with the slight reduction in the wear coefficient, as detailed in Fig. 7. The comparatively limited total disc wear, owing to the short duration of the pin-on-disc tests, is further compensated by the disc weight increase due to the sticking of the wear debris from the pin.

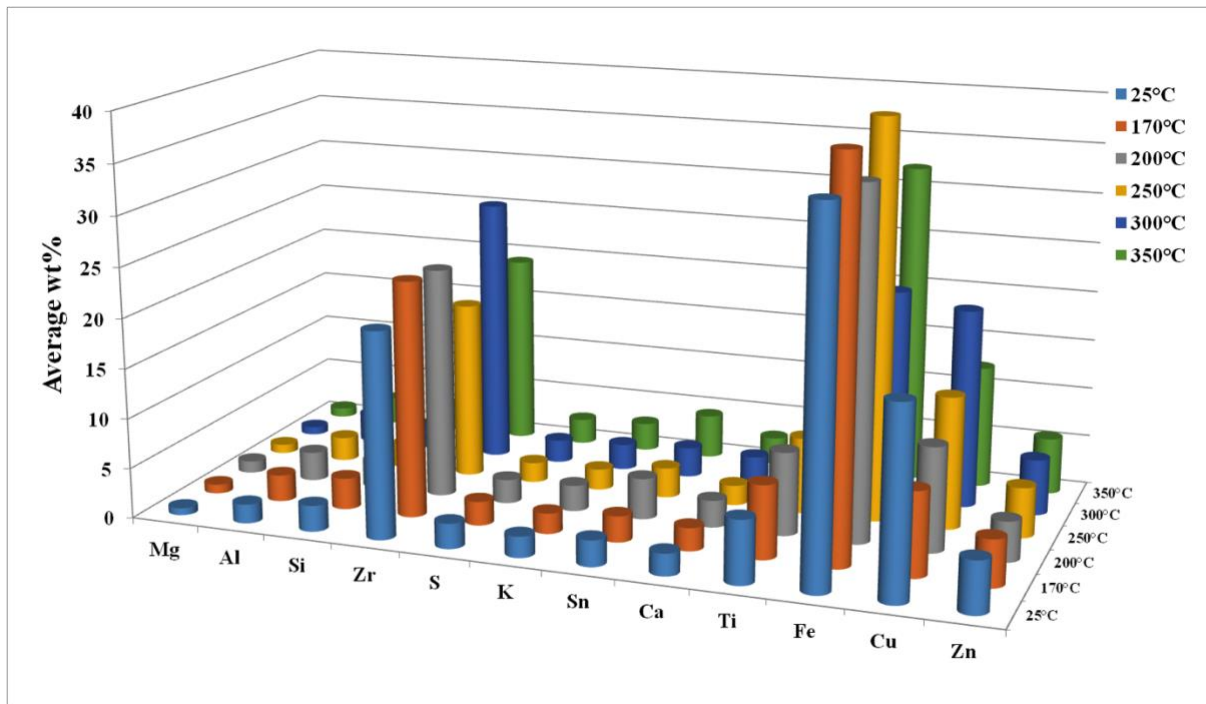


Figure 12: Average elemental composition of wear debris on disc surface.

5. Conclusions

The focus of this work is the wear behavior as a function of the temperature of a brake pad friction material, investigated by pin-on-disc tests, using a cast iron disc as counterface. Tests were conducted at disc temperatures ranging from 25°C (room temperature) up to a maximum of 350°C, in order to study how the thermal evolution of the components of the friction material, in particular the decomposition of the organic binder, influences the main wear mechanisms. These were inferred from the analyses of the wear tracks left after the tests on the surface of the pin and disc specimens. Raman spectroscopy and SEM coupled with EDXS were the main experimental tools used for this purpose. The following main conclusions can be drawn from this work:

- According with TGA results and in agreement with literature data, the thermal decomposition of the phenolic binder in the friction material takes place in two main steps. A first minor mass reduction (0.04%) appears at 90°C and major decomposition (3.77%) starts at about 280°C with a maximum decomposition rate at 415°C.
- At high temperatures, carbonaceous products are present on worn surfaces of the pin specimens as proved by Raman spectroscopy results.

- These carbonaceous products are the result of the thermal decomposition of the phenolic binder present in the pin material, although the influence of frictional heating and shear stresses associated with the tribological tests have certainly influenced the decomposition kinetics.
- A transition in wear rate from mild to severe wear is observed when disc temperature is increased from 170°C to 200°C.
- The mild wear regime is determined by the presence of a stable friction layer forming on the pin surface. This layer has a standard composite microstructure, made of the so-called primary and secondary plateaus. The first ones are made of the hard and tough pin components, like ceramic particles and metallic fibers, protruding from its surface after the early run-in stage. The secondary plateaus result from the accumulation of wear debris, also coming from the tribo-oxidation of the disc, that under favourable conditions form a compact and protective layer.
- At high temperatures, the severe wear is determined by the decomposition of phenolic resins present in the pin material, which leads to low debris retention and low residence time for the formation of an effective wear protective layers.
- In particular, nearly no secondary plateaus form on the pin surface at 350°C and an important abrasive wear of the disc takes place, as proved by increasing values of the friction coefficient.
- In general, the composition of the friction layers observed at different temperatures and their stability are paramount to infer the composition of the particles and fragments emitted by this sort of tribological systems.

In addition, under extreme conditions, compared to those faced in real brake systems, the study highlights some critical aspects of the tribological behavior of brake materials that can be taken into account in developing better performing brake systems, that eventually will have to be tested under real conditions for an effective assessment of their performances [33].

Acknowledgements

The research leading to these results has achieved funding from the European Union Seventh Framework Programme (FP-PEOPLE-2012-IAPP) under the Rebrake Project, grant agreement no. 324385 (www.rebrake-project.eu). The Authors wish to thank Guido Perricone (Brembo S.p.A.) for useful discussions; Gloria Ischia and Lorena Maines for wear testing and characterization support.

References

- [1] G. Straffelini, Friction and wear, methodologies for Design and Control, Springer, 2015.
- [2] N.S.M. EL-Tayeb, K.W. Liew, V.C. Venkatesh, Evaluation of new frictional brake pad materials. Proc. International Conference on Manufacturing Science and Technology, Malacca-Malaysia, 28-30 August (2006) 380-383.
- [3] A.E. Anderson, Brake system performance-effect of fiber types and concentrations Proceedings of fibers in linings symposium, The Asbestos Institute, Montreal, Quebec (1987) 2-57.
- [4] M.G. Jacko, P.H.S. Tsang, S.K. Rhee, Automotive linings evolution during the past decade, Wear 100 (1984) 503-515.
- [5] P.V. Gurunath, J. Bijwe, Friction and wear studies on brake-pad materials based on newly developed resin, Wear 263 (2007) 1212-1219.

- [6] S.J. Kim, H. Jang, Friction and wear of friction materials containing two different phenolic resins reinforced with aramid pulp, *Tribol. Intern.* 33 (2000) 477-484.
- [7] S. Ramousse, J.W. Hoj, O.T. Sørensen, Thermal characterization of brake pads, *J. Therm. Anal. Calorim.* 64 (2001) 933-943.
- [8] K. Bode, G.P. Ostermeyer, A comprehensive approach for the simulation of heat and heat-induced phenomena in friction materials, *Wear* 311 (2014) 47-56.
- [9] A. Wirth, D. Eggleston, R. Whitaker, A fundamental tribochemical study of the third body layer formed during automotive friction braking, *Wear* 179 (1-2) (1994) 75-81.
- [10] J. Jiang, F.H. Stott, M.M. Stack, A mathematical model for sliding wear of metals at elevated temperatures, *Wear* 181-183 (1995) 20-31.
- [11] J. Jiang, F.H. Stott, M.M. Stack, The effect of partial pressure of oxygen on the tribological behavior of a nickel-based alloy, N80A, at elevated temperatures, *Wear* 203-204 (1997) 615-625.
- [12] J. Jiang, F.H. Stott, M.M. Stack, The role of triboparticulates in dry sliding wear, *Tribol. Intern.*, 31 (1998) 245-256.
- [13] G. Straffelini, A simplified approach to the adhesive theory of friction, *Wear* 249 (2001) 78-84.
- [14] W. Osterle, I. Urban, Third body formation on brake pads and rotors, *Tribol. Intern.* 39 (2006) 401-408.
- [15] W. Osterle, I. Urban, Friction layers and friction films on PMC brake pads, *Wear* 257 (2004) 215-226
- [16] P. Filip, Z. Weiss, D. Rafaja, On friction layer formation in polymer matrix composite materials for brake applications, *Wear* 252 (2002) 189-198.
- [17] M. Eriksson, S. Jacobson, Tribological surfaces of organic brake pads, *Tribol. Intern.* 33 (2000) 817-827.
- [18] M.G Jacko, P.H.S Tsang, S.K Rhee, Wear debris compaction and friction film formation of polymer composites, *Wear* 133 (1989) 23-38.
- [19] K. Bode, G.-P. Ostermeyer, A comprehensive approach for the simulation of heat and heat-induced phenomena in friction materials, *Wear* 311 (2014) 47-56.
- [20] M. Eriksson, J. Lord, S. Jacobson, Wear and contact conditions of brake pads: dynamical in situ studies of pad on glass, *Wear* 249 (2001) 272-278.
- [21] P. C. Verma, L. Menapace, A. Bonfanti, R. Ciudin, S. Gialanella, G. Straffelini, Braking pad-disc system: Wear mechanisms and formation of wear fragments, *Wear* 322-323 (2015) 251-258.
- [22] M. Patel, C. L. Azanza Ricardo, P. Scardi, P.B. Aswath, Morphology, structure and chemistry of extracted diesel soot—Part I: Transmission electron microscopy, Raman spectroscopy, X-ray photo electron spectroscopy and synchrotron X-ray diffraction study, *Tribol. Intern.* 52 (2012) 29-39.
- [23] G.M. Ingo, M. D'Uffizi, G. Falso, G. Bultrini, G. Padeletti, Thermal and microchemical investigation of automotive brake pad wear residues, *Thermoch. Acta* 418 (2004) 61-68.

- [24] F. Eddoumy, H. Kasem, H. Dhieb, J. G. Buijnsters, P. Dufrenoy, J.-P. Celis, Y. Desplanques, Role of constituents of friction materials on their sliding behavior between room temperature and 400°C, *Materials and Design* 65 (2015) 179-186.
- [25] F. Georges, J. Sykes, Decomposition characteristics of a char-forming phenolic polymer used for ablative composites, *Nat. Aeronautics Space Admin.* (1967) NASA TN D-3810.
- [26] J. Bijwe, N. Majumdar, B.K. Satapathy, Influence of modified phenolic resins on the fade and recovery behavior of friction materials, *Wear* 259 (2005) 1068-1078.
- [27] U.S. Hong, S.L. Jung, K.H. Cho, Cho M.H., Kim S.J., Jang H, Wear mechanism of multiphase friction materials with different phenolic resin matrices, *Wear* 266 (2009) 739-744.
- [28] M. Eriksson, F. Bergman, S. Jacobson, Surface characterization of brake pads after running under silent and squealing conditions, *Wear* 232 (1999) 163-167.
- [29] M. Eriksson, F. Bergman, S. Jacobson, On the nature of tribological contact in automotive brakes, *Wear* 252 (2002) 26-36.
- [30] W. Osterle, M. Griepentrog, Th. Gross, I. Urban, Chemical and microstructural changes induced by friction and wear of brakes, *Wear* 251 (2001) 1469-1476.
- [31] W. Osterle, C. Prietzel, H. Kloß, A.I. Dmitriev, On the role of copper in brake friction materials, *Tribol. Intern.* 43 (2010) 2317-2326.
- [32] A. Cuesta, P. Dhamelinourt, J. Laureyns, A. Martinez-Alonso, J.M.D. Tascon, Raman microprobe studies on carbon materials, *Carbon* 32 (1994) 1523-1532.
- [33] H. Hagino, M. Oyama, S. Sasaki, Airborne brake wear particle emission due to braking and accelerating, *Wear*, 334-335 (2015) 44-48.